

# Genotoxicity, biochemical, and biodistribution studies of magnesium oxide nano and microparticles in albino wistar rats after 28-day repeated oral exposure

Bhanuramya Mangalampalli<sup>1,2</sup> | Naresh Dumala<sup>1,2</sup> | Rekha Devi Perumalla Venkata<sup>1</sup> | Paramjit Grover<sup>1</sup> 

<sup>1</sup>Toxicology Unit, Pharmacology and Toxicology Department, CSIR - Indian Institute of Chemical Technology, Hyderabad, Telangana 500007, India

<sup>2</sup>Academy of Scientific and Innovative Research, CSIR - Indian Institute of Chemical Technology, Hyderabad, Telangana 500007, India

## Correspondence

Paramjit Grover, CSIR-Emeritus Scientist, Toxicology Unit, Pharmacology and Toxicology Division, CSIR - Indian Institute of Chemical Technology, Hyderabad 500007, Telangana, India.  
Email: paramgrover@gmail.com (or) grover@iict.res.in

## Funding information

Director IICT, Hyderabad; University Grants Commission; Council of Scientific and Industrial Research, India

## Abstract

Increased utilization and exposure levels of Magnesium oxide (MgO) nanoparticles (NPs) to humans and environment may raise unexpected consequences. The goal of this study was to evaluate the toxicological implications of MgO NPs and MPs after 28 day repeated oral administration in Wistar rats with three different doses (250, 500, and 1000 mg/kg). The MgO particles were characterised systematically in order to get more insights of the toxicological behaviour. MgO NPs induced significant DNA damage and aberrations in chromosomes. Moreover, hepatic enzymes released into the systemic circulation caused significant elevated levels of physiological enzymes in blood. NPs could interfere with proteins and enzymes and alter the redox balance in cell environment. Significant accumulation of Mg in all tissues and clearance via urine and faeces was noted in size dependent kinetics. Oral administration of MgO NPs altered the biochemical and genotoxic parameters in dose dependent and gender independent manner.

## KEYWORDS

biotransformation, genotoxicity, hematological alterations, histopathology, nanoparticles, oxidative stress

## 1 | INTRODUCTION

Magnesium oxide (MgO) NPs have been used in diverse fields including electronics, catalysis, ceramics industries, and synthesis of petrochemical products, coatings as well as biomolecular detection and diagnostics.<sup>1</sup> These NPs are also found to be useful in materials for soundproofing, heat-insulating, refractory fiberboard, and metallic ceramics. Further, MgO NPs are frequently employed as fuel additives, antistatic

agent, and corrosion inhibitors in the chemical industry.<sup>2</sup> The antibacterial and cytotoxic effects of MgO NPs have been investigated on *Vibrio Cholerae* bacterial strains and human intestinal and cervical cancer cell line. The results revealed significant antibacterial and anticancer properties.<sup>3</sup> Increased utilisation of these NPs has a direct (proportional) relation to the human exposure levels. Investigations conducted with MgO NPs using *in vitro* models revealed conflicting results. In a study on human umbilical vein endothelial cells (HUVECs) proliferation, MgO NPs significantly enhanced the nitric oxide release and total antioxidant competence content of the HUVECs.<sup>4</sup> Another study on human cardiac microvascular endothelial cells (HCMECs) with MgO NPs showed concentration and time-dependent cytotoxicity. The MgO NPs also elicited permeability and inflammation response in HCMECs.<sup>5</sup> However, MgO NPs were found to be least effective in inducing cell death in human astrocytoma U87 cells.<sup>6</sup> Another study conducted on human liver epithelial cancer cell line for genotoxic effects of MgO NPs, did not produce significant effects compared with control

**Abbreviations:** ALP, alkaline phosphatase; ALT, alanine aminotransferase; ANOVA, analysis of variance; AST, aspartate aminotransferase; BET, Brunner-Emmett-Teller technique; DLS, dynamic light scattering; ICP-OES, inductively coupled plasma optical emission spectrometer; LDV, laser doppler velocimetry; MgO MPs, magnesium oxide microparticles; MgO NPs, magnesium oxide nanoparticles; MI, mitotic index; MN-PCE, micronucleated polychromatic erythrocytes; MNT, micronucleus test; OECD, organization for economic cooperation and development; % PCE, percentage of polychromatic erythrocytes; ROS, reactive oxygen species; TEM, transmission electron microscopy; XRD, X-ray diffraction.

experiments at the investigated concentrations.<sup>7</sup> A few *in vivo* investigations with MgO NPs are available. A study conducted with MgO NPs and MPs on Wistar rats produced dose-dependent acute oral toxicity.<sup>8</sup> Another study reported on MgO NPs produced pulmonary toxicity after acute intratracheal instillation.<sup>9</sup> A study reported on the antioxidant status in serum of rats after acute intratracheal instillation of MgO NPs. The results revealed oxidative stress due to the reduction in total antioxidant capacity.<sup>10</sup> However, the consequences of repeated/chronic exposure to these NPs have not yet been explored. It is estimated that of all the NPs in consumer products, applications of MgO NPs currently have the special place in biomedical and chemical industry. Despite the great promise the MgO NPs have for the future medical applications their complete toxicological profile has not been reported. Therefore, keeping in view the lack of toxicological data and to evaluate the risk/benefits ratio for the use of MgO NPs in any technological or medical developments, this study was accomplished. Understandably, the matter of safety and toxicity has become an issue of interest to the public. Therefore, understanding the interactions of these MgO NPs with biological systems is a particularly important scientific issue discussed in this study. Thus, there is an urgent need to develop rapid, accurate, and efficient testing strategies to assess toxic effects of these particles on humans. Toxicity data generated in this study will be useful in predicting the possible toxic hazards that may arise from the introduction of MgO NPs and MPs into the environment.

The measured toxicological endpoints of NPs are valid only when the particles are characterized extensively.<sup>11</sup> Further, physicochemical characterization of NPs prior to the toxicological assessment is important to understand the biological behavior upon entry, as physical and chemical properties of particles are likely to play a vital role in their potential toxicity. Hence, MgO NPs and MPs were characterized using transmission electron microscopy (TEM) for particle size and morphology assessment. Dynamic light scattering (DLS) analysis was performed for average hydrodynamic diameter and size distribution of the particles in Milli-Q water. Laser Doppler velocimetry (LDV) was used for zeta potential as well as for determining electrophoretic mobility. Brunner–Emmett–Teller (BET) analysis was carried out for surface area measurements. Genotoxicity studies are important for safety assessment and environmental biomonitoring of NPs for understanding the possible mutations and cancer risk upon exposure. Further, the frequently observed paradigms for NP-mediated toxicity include oxidative stress and genetic damage.<sup>12</sup> Production of reactive oxygen species (ROS) upon exposure to NPs is being considered as the primary underlying cause of nano toxicology, which in turn leads to DNA damage and even cell death.<sup>13,14</sup> Hence, the genotoxicity of the MgO NPs and MPs was assessed by comet assay in peripheral blood leukocytes (PBL), liver and bone marrow, micronucleus test (MNT) in bone marrow cells and peripheral blood (PB) and chromosomal aberrations (CAs) test in the bone marrow cells to determine mitotic index (MI) and aberrations of chromosomes. Malondialdehyde (MDA), which is the end product of lipid peroxidation, reduced glutathione (GSH), lactate dehydrogenase (LDH), catalase (CAT) profiles were determined in serum and liver, kidney homogenates for hepatic and renal toxicity. The levels of these enzymes are gross measures of protein status and reflect significant

changes in liver and kidney functions. Biochemical parameters such as alkaline phosphatase (ALP), aspartate aminotransferase (AST), alanine aminotransferase (ALT) were measured. Hematological markers like the count of red blood cells (RBC), white blood cells (WBC), hemoglobin (HGB), hematocrit (HCT), and mean corpuscular volume (MCV) were estimated. Histopathological examination is necessary to determine the alterations in tissue architecture due to NPs exposure and for assessing the toxicological effects. Biotracking of the tested materials gives valuable information on organ specificity, uptake, retention, and clearance patterns. Hence, the metal content analysis is essential to know their anatomic fate after biodistribution. The amount of metal content in rat's whole blood, liver, kidney, spleen, heart, brain, urine, and feces was estimated using inductively coupled plasma optical emission spectrophotometry (ICP-OES) method.

## 2 | MATERIALS AND METHODS

### 2.1 | Chemicals

MgO nano powder (MgO < 60 nm, product no. 549649, CAS No. 1309-48-4) and low-melting point agarose, normal-melting point agarose were purchased from Sigma-Aldrich Chemical (St Louis, MO). MgO MPs (fine powder, GRM1031, CAS No. 1309-48-4) as per the manufacture's data sheet, ethylene diamine tetra-acetic acid (EDTA) disodium salt, phosphate buffered saline ( $\text{Ca}^{2+}$ ,  $\text{Mg}^{2+}$  free), Giemsa stain and all other chemicals used in the current study were purchased from Himedia, Mumbai, India.

### 2.2 | NPs and MPs suspensions preparation

The MgO NPs and MPs were suspended in deionized water (DI water) and dispersed by ultrasonic vibration (UPH 100; Hielscher Ultrasonics GmbH, Teltow, Germany, 30 kHz) for 10 min to produce different concentrations at 250, 500, and 1000 mg/kg.

### 2.3 | Characterization of particles

The particles were characterised to obtain size and morphology by using TEM analysis (at 120 kV). The size distribution of NPs and state of agglomeration in Milli-Q water were measured by DLS and LDV using a Malvern Instruments Zetasizer Nano-ZS Instrument. The polydispersity index (Pdl) was used to measure the size ranges present in the NPs dispersion. The specific surface area ( $\text{m}^2 \text{g}^{-1}$ ) of the MgO NPs and MPs was measured by BET method (Quadrasorb-SI V 5.06 instrument (M/S Quanta chrome Instruments Corporation, Boynton Beach, FL). The X-ray diffraction (XRD) patterns of the MgO particles were documented on a Bruker AXS D-8 Advance powder X-ray diffractometer (Shimadzu, Japan).

### 2.4 | Animals for *in vivo* study

Male and female Wistar rats of 8–12 week old were procured from National Institute of Nutrition, Hyderabad, India. The rats were allowed to acclimatise for a week in standard polypropylene cages before the start of the experiment. The body weight (bw) of the animals at the

beginning of the study was 120–140 g. The rats were housed conventionally with a 12 h light/dark cycle, room temperature was  $22 \pm 3^\circ\text{C}$  and the relative humidity was 55–65%. The animals were fed a standard pellet diet and provided tap water ad libitum. The animal study was performed under the conditions approved by Institutional Animal Ethics Committee, and the approval no. was IICT/BIO/TOX/PG/25/06/2014/08.

## 2.5 | Treatment of animals

MgO-NPs and MPs were suspended in Milli-Q water, properly ultrasonicated and then vortexed before every treatment of the rats. A 28 day repeated dose oral toxicity study was conducted with male and female Wistar rats. A preliminary study on acute oral study of MgO NPs and MPs was carried out initially.<sup>8</sup> In this study, three doses (low, medium, and high) were selected based on our previous investigation. The highest dose was selected based on induction of toxic effect without severe sufferings and mortality, whereas the lowest dose demonstrated no observed adverse effect levels. Further, a descending sequence of dose levels (500 and 250 mg/kg bw/day) was selected with a view to demonstrate any dosage-related response as per OECD guideline 407.<sup>15</sup> The animals were divided into four groups (10 rats; 5 males and 5 females in each group). Control (Milli-Q water), low dose (250 mg/kg bw/day), medium dose (500 mg/kg bw/day), and high dose (1000 mg/kg bw/day) of NPs and MPs treated daily using oral gavage. The feed intake and bw were monitored daily during the observation period. Recordings were made regularly for mortality, signs, and symptoms if any. At the end of the test period, the animals were sacrificed by cervical dislocation 24 h after the administration of the last dose. The various tissues from the rats after sacrifice were collected for biochemical, genotoxic, histopathology, and metal content analysis. Ethyl methanesulfonate (EMS), a known mutagen, was used as the positive control for genotoxicity studies at a dose of 200 mg/kg bw, and the volume injected was 0.01 mL/g bw [given intraperitoneally (ip) 24 h before sacrifice]. For genotoxicity analysis, all the microscopic slides were scored blindly to avoid bias.

## 2.6 | Genotoxicity parameters

### 2.6.1 | Comet assay (single cell gel electrophoresis)

The alkaline comet assay in male and female Wistar rats treated with MgO-NPs and MPs after 28-day repeated oral dosing with various doses was conducted for the assessment of DNA damage in PBL, liver, and bone marrow cells.<sup>16,17</sup> Cell viability was determined by the trypan blue exclusion assay.<sup>18</sup> Three slides were prepared for each experimental point. The slides were analysed by staining with ethidium bromide (20  $\mu\text{g/mL}$ ) using a fluorescence microscope (Olympus, Shinjuku-ku, Tokyo, Japan) and 50 randomly selected comets (cells) per slide (150 cells per rat) were analysed to estimate the amount of DNA damage. Quantification of DNA breakage was carried out by using CASP software version 1.2.2 (Comet Assay Software, CaspLab) to calculate the amount of DNA damage and expressed as a percentage of DNA in the comet tail.

### 2.6.2 | Micronucleus test

The MNT was performed in the bone marrow cells, which were extracted from femur and tibia of the rats by aspiration as per protocol

of OECD TG 474 and Schmid.<sup>19,20</sup> The extractions were placed in a hypotonic solution made of 1% sodium citrate and centrifuged to get a pellet. The pellet was resuspended in 1% sodium citrate and used to prepare smears on microscopic slides and dried overnight in humidified air. Whole blood was collected from the retro-orbital plexus of rat and smears were made and allowed to dry. The air-dried slides were fixed in methanol and stained with 0.5% Giemsa for 3–5 min. The stained slides were used for assessing the occurrence of micronuclei (MN). Three slides were made for each animal and microscopically examined at  $\times 1000$  magnification; 2000 polychromatic erythrocytes (PCE) per animal were assessed from the three slides and the micronucleated PCEs frequency (MN-PCE) was recorded.

### 2.6.3 | CA assay

The method described in OECD TG 475<sup>21</sup> was used as a test method to carry out CA analysis in bone marrow cells after 28 day repeated oral treatment with the various doses of MgO NPs and MPs. For analysis of metaphase cells, cell division was arrested by a mitotic inhibitor (colchicine, 0.02%) which was injected ip 2 hr prior to sacrifice. The bone marrow was collected from femur and tibia by rinsing in a hypotonic solution (0.56% potassium chloride) and centrifuged. Cells were then fixed in fixative i.e. ice-cold Carnoy's solution (methanol: acetic acid, 3:1 V/V) until the pellets were clean. After overnight refrigeration, cells were centrifuged and resuspended in Carnoy's solution, dropped onto slides, dried and stained with Giemsa. Three slides for each animal were prepared by the flame-dried technique. Five hundred well-spread metaphases per dose (100/animal) were selected to detect the presence of CAs. One thousand cells were examined for determining MI.

## 2.7 | Biochemical assays

### 2.7.1 | Blood sampling and tissue processing

Blood samples were collected from all the control and treated animals for complete blood picture and biochemical analysis as well. Blood was collected by puncturing the retro-orbital sinus into heparin-coated capillaries. Before taking the blood, animals were anaesthetized with an optimal cocktail of xylazine and ketamine to avoid pain/distress. A small amount (0.5 mL) of blood was collected in 10% EDTA coated vials for hematological parameters and serum was collected by centrifuging blood without any anticoagulant for biochemical analysis. Tissues such as the liver and kidney of both control and treated rats were dissected out and quickly homogenized separately in ice-cold homogenization buffer using a Micra D-1-high speed tissue homogenizer to make 10% homogenate (W/V). To get the supernatant, the homogenate was centrifuged at 12 000 rpm for 10 min. The collected supernatants along with the serum were stored in  $-20^\circ\text{C}$  freezer until use for the biochemical analysis. The levels of various enzymes like ALP, AST, and ALT were assessed according to the method of Yatzidis.<sup>22</sup> The levels of CAT, GSH, MDA, and LDH were estimated by the standard protocols,<sup>23–26</sup> respectively.

## 2.8 | Histopathology

Histopathology of the stomach, liver, kidney, spleen, and brain was carried out in control and treated rats post oral exposure to MgO NPs and

TABLE 1 Characterization of MgO NPs and MPs

Particles	Size using TEM	DLS		LDV			Surface area (m <sup>2</sup> g <sup>-1</sup> )
		Average diameter (nm)	PDI	Zeta potential (mV)	Electrophoretic mobility (μm cm)/(V s)	pH	
MgO NPs (nm)	59.85 ± 5.72	191.82 ± 21.5	0.304	-10.5	0.0308	7.0	142.8 ± 3.52
MgO MPs (μm)	7.47 ± 1.17	ND	ND	ND	ND	7.0	43.88 ± 2.35

MgO NPs and MPs at the concentration of 40 μg/mL were dispersed in Milli-Q water and mixing was done via probe sonication for 10 min just before estimations.

Abbreviations: Pdl, polydispersity index; DLS, dynamic light scattering; LDV, laser doppler velocimetry; ND, not detectable.

MPs for 28 days. After sacrifice, the tissues were washed with 1% cold saline to remove excess blood and tissue debris and then fixed in neutral buffered 10% formalin. The tissues were processed with a tissue processor and embedded in paraffin blocks, then trimmed and sectioned using a microtome. Paraffin sections of 3 μm thickness were stained with hematoxylin & eosin and mounted on a glass microscope slide. Three random sections per organ were examined with Nikon Eclipse E 800 microscope at ×400 magnification for histological alterations.

## 2.9 | Mg content analysis in tissues

Biodistribution analysis of the MgO NPs and MPs in the male and female Wistar rats was carried out after 28 days of repeated oral treatment. The animals were placed in metabolic cages to collect the urine and faeces samples at the end day of every week during the study period. Whole blood, liver, kidneys, heart, brain, and spleen were taken after sacrificing the rats after the 28 day of the treatment. For elemental analysis, all the samples were processed by following the methods described by standard protocols.<sup>8,27</sup> Briefly, 0.3 g of fresh tissue and faeces samples and 0.3 mL of blood and urine samples were predigested in nitric acid (70%) overnight. The samples were then heated at 80°C for 10 h followed by additional heating at 130–150°C for 30 min. Finally, 0.5 mL of 70% perchloric acid was added to all the samples, and they were again heated for 4 h for evaporation nearly to dryness. After tissue digestion, the samples were filtered and made up to 15 mL using 2% HNO<sub>3</sub> for analysis. The Mg content in the samples was determined by ICP-OES.

## 2.10 | Statistical analysis

The significant changes were analysed statistically by two-way ANOVA. Results were expressed as the mean ± standard deviation (SD). Multiple comparisons were performed using the Bonferroni post-test. All calculations were performed using Graph Pad Prism 5 software package for Windows (GraphPad Software, La Jolla, CA). The statistical significance for all tests was set at  $P < .05$ .

# 3 | RESULTS

## 3.1 | Characterization of MgO NPs and MPs

The physical characteristics of MgO particles were determined by TEM, DLS, LDV, and BET analysis and the results obtained are shown in Table 1. The average particle size of MgO NPs and MPs was found to be

59.85 ± 5.72 nm and 7.47 ± 1.17 μm (Figure 1A,B), respectively. The hydrodynamic diameter and Pdl of MgO NPs in Milli-Q water suspension obtained by DLS was (191.82 ± 21.5) nm and 0.304, respectively. The agglomeration phenomenon may be the reason behind the larger hydrodynamic diameter for MgO NPs in Milli-Q water suspension than the TEM size of NPs in the dry state. The XRD pattern of NPs revealed a pure hexagonal shape, whereas MPs were cubic in nature (Figure 1C). The specific surface area of MgO NPs and MPs was found to be 142.8 ± 3.52 and 43.88 ± 2.35 m<sup>2</sup>/g by BET analysis. Zeta potential (ζ) and electrophoretic mobility of MgO NPs in Milli-Q was quantified by LDV and found to be -10.5 mV and 0.0308 (μm.cm)/(V.sec), respectively, at pH 7.0 (Figure 1D,E), whereas MgO MPs were not detected in the LDV analysis.

## 3.2 | Animal observation, food consumption, bw, and organ weight

After 28 days repeated oral dosing with MgO NPs and MPs to male and female Wistar rats, mortality was not observed in any of the treated groups. However, rats, which received high dose of MgO NPs showed dullness, irritation, and moribund symptoms. Further, both MgO NPs and MPs treated animals showed decrease in feed intake, bw, and relative organ weight (Figure 2). The percentage (%) decrease in feed intake was in the range of 13.0–20.5% in MgO NPs treated group and 1.7–12.4% in MPs treated group. Likewise, % bw loss was in the range of 10.9–16.7 and 8.0–10.2% in NPs and MPs exposed rats, respectively.

## 3.3 | Hematological estimations

The hematological results revealed that the RBC, HGB, HCT, MCV, and PLT values of the MgO NPs and MPs treated male and female rats were reduced. However, WBC of the rats was elevated with increasing doses of NPs and MPs compared with control groups of both the sexes. Further, the change was significant ( $P < .05$ ) only in rats treated with 1000 mg/kg MgO NPs (Table 2).

## 3.4 | Genotoxicity analysis

### 3.4.1 | Comet assay

The findings of the comet assay in PBL, liver and bone marrow cells of male and female Wistar rats after 28 days repeated oral treatment with MgO NPs and MPs are depicted in Figure 3A,B. In all the samples, the cell viability was determined by the Trypan blue exclusion assay and



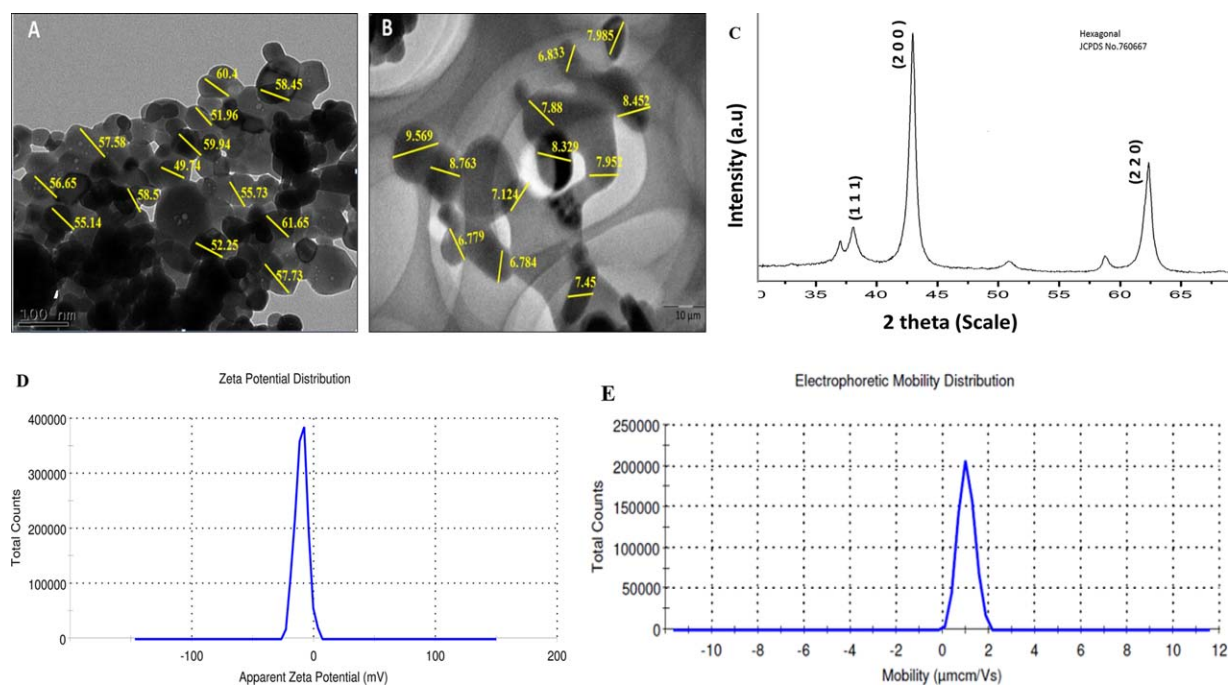


**FIGURE 1** TEM image of (A) MgO NPs and (B) MgO MPs in Milli-Q water for characterization of particles. C, XRD spectrum (The peak positions were corresponding to the standard XRD patterns of MgO NPs (JCPDS file 760667). D, Zeta potential. E, Electrophoretic mobility of MgO NPs [Color figure can be viewed at [wileyonlinelibrary.com](http://wileyonlinelibrary.com)]

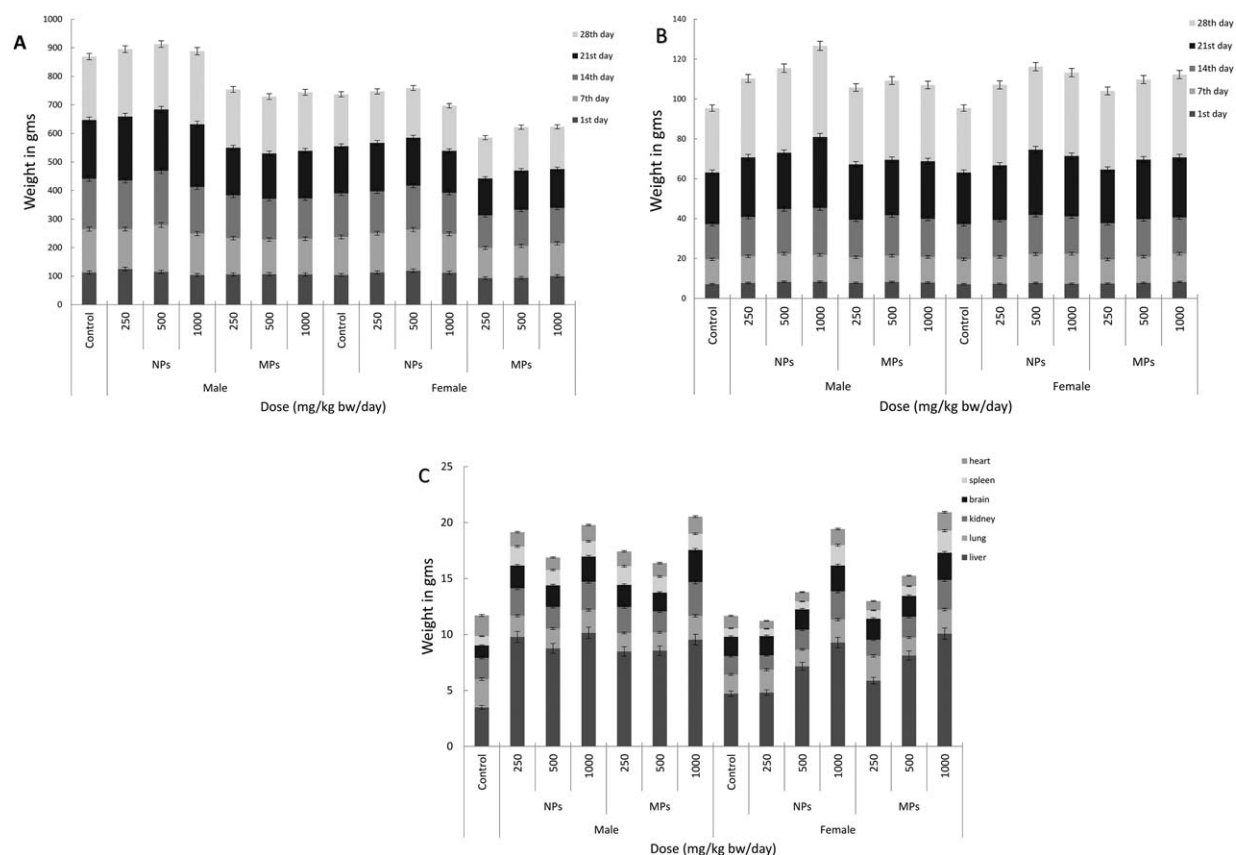


**FIGURE 2** A, Feed-intake; B, bw, and C, relative organ weight profile of control and treated male and female rats

was > 90% (data not shown). The results revealed a significant increase in % tail DNA at high dose of MgO NPs and MPs ( $P < .01$ ) in PBL, liver, and bone marrow cells. However, at the low dose of NPs and low and medium doses of MPs the results were nonsignificant. The mean % tail DNA of positive control treated rats was significant ( $P < .01$ ) when compared with the control groups in both the sexes. Moreover, gender-dependent variation in % tail DNA was not evident.

### 3.4.2 | Micronucleus test

The MNT in bone marrow and PBL cells of male and female Wistar rats revealed a dose dependent clastogenic effect. There was an increment in MN-PCE frequency in bone marrow and PB cells (Table 3) of rats, which received MgO NPs in dose dependent pattern. The effect was significant ( $P < .01$ ) at 1000 and ( $P < .05$ ) at 500 mg/kg. MgO MPs treated groups also showed a dose-related increase in the number of MN-PCE; however, the increase was nonsignificant at low and medium doses. However, the positive control group of rats treated with EMS showed significant ( $P < .01$ ) enhancement in MN-PCE frequency and % PCEs as well when compared with the controls.

### 3.4.3 | CA assay

The results of the CA assay in bone marrow cells of male and female Wistar rats treated with MgO NPs and MPs are shown in Table 4. The MI did not reveal any significant differences between treated and control groups. Total cytogenetic changes including gaps, breaks, minutes, acentric fragments and aneuploidy were observed at 1000 and 500 mg/kg MgO NPs treated rats and found to be significant at  $P < .01$ . However, there was a dose-dependent increase in numerical and structural changes in treated groups of rats compared to controls. There were no changes in polyploidy level and reciprocal translocations in any treated dose level except in EMS treated a group of rats. The total cytogenetic changes induced by EMS were highly significant in both the genders of rats when compared with the treated groups and respective controls.

## 3.5 | Biochemical alterations

Biochemical indices were determined in the male and female Wistar rats, which received various doses of MgO NPs and MPs after 28 days repeated oral treatment. The levels of AST and ALT in serum at the dose of 1000 mg/kg for MgO NPs were significantly increased ( $P < .01$ ), whereas at low and medium doses and all the doses of MPs, the respective enzyme levels were increased in a dose-dependent manner but the increase was nonsignificant in both the sex of rats (Table 5). Significantly elevated levels of ALP in serum, liver, and kidney homogenates were observed at 1000 mg/kg doses of NPs ( $P < .01$ ), whereas, at low dose of NPs and low and medium doses of MPs the increase was non-significant. The MDA and LDH levels were significantly increased, where as, GSH and CAT levels were decreased in rats receiving high dose of MgO NPs in both male and female rats in liver as well as kidney homogenates (Tables 6 and 7). At 250 and 500 mg/kg dose of MgO NPs and all the doses of MPs, an enhancement in the level of MDA and the slight decrease in the levels of GSH and CAT was observed, which was nonsignificant compared with control group of rats.

TABLE 2 Hematological parameters observed in male and female Wistar rats treated repeatedly for 28 days with different doses of MgO NPs and MPs

Hematology parameters	Male					Female								
	Control	MgO NPs			MgO MPs			Control	MgO NPs			MgO MPs		
		Milli-Q	250	500	1000	500	1000		250	500	1000	250	500	1000
WBC 103/ $\mu$ L	10.16 $\pm$ 2.85	12.1 $\pm$ 1.2	13.4 $\pm$ 1.43	14.88 $\pm$ 1.34	9.58 $\pm$ 1.5	10.18 $\pm$ 1.3	11.56 $\pm$ 2.32	10.16 $\pm$ 2.5	11.2 $\pm$ 2.5	12.3 $\pm$ 2.43	13.8 $\pm$ 1.34	9.18 $\pm$ 1.5	10.48 $\pm$ 1.3	11.96 $\pm$ 1.32
RBC 106/ $\mu$ L	2.27 $\pm$ 1.15	2.75 $\pm$ 0.5	3.07 $\pm$ 1.4	3.85 $\pm$ 1.43	3.68 $\pm$ 1.8	3.43 $\pm$ 1.87	3.66 $\pm$ 1.76	1.27 $\pm$ 0.75	1.75 $\pm$ 0.3	2.07 $\pm$ 0.4	3.25 $\pm$ 0.43	1.98 $\pm$ 0.8	2.13 $\pm$ 0.87	2.66 $\pm$ 0.76
HGB gm/dL	11.76 $\pm$ 0.96	12.1 $\pm$ 0.54	13.8 $\pm$ 1.2	14.4 $\pm$ 2.1a	10.92 $\pm$ 1.66	11.72 $\pm$ 1.76	12.72 $\pm$ 1.65	11.76 $\pm$ 1.6	12.6 $\pm$ 1.54	13.4 $\pm$ 1.2	14.4 $\pm$ 2.1a	11.92 $\pm$ 1.66	12.12 $\pm$ 1.76	12.72 $\pm$ 1.65
HCT %	12.8 $\pm$ 1.6	13.6 $\pm$ 1.2	14.2 $\pm$ 2.4	15.45 $\pm$ 2.6	12.46 $\pm$ 3.06	13.08 $\pm$ 1.5	13.14 $\pm$ 2.6	12.3 $\pm$ 1.6	13.8 $\pm$ 1.2	14.6 $\pm$ 2.1	15.4 $\pm$ 3.1	12.96 $\pm$ 0.6	13.18 $\pm$ 0.5	14.14 $\pm$ 0.6
MCV $\mu$ /m <sup>3</sup>	60 $\pm$ 15.36	61 $\pm$ 12.1	62 $\pm$ 12.54	73 $\pm$ 13.21	59.6 $\pm$ 11.2	63.8 $\pm$ 11.6	65.8 $\pm$ 11.7	57 $\pm$ 11.7	61 $\pm$ 12.1	64 $\pm$ 12.54	69 $\pm$ 13.21	57.6 $\pm$ 11.2	60.8 $\pm$ 11.6	66.8 $\pm$ 11.7
PLT 103/ $\mu$ L	88.6 $\pm$ 17.8	90 $\pm$ 20.1	98 $\pm$ 24.62	104 $\pm$ 18.1	89 $\pm$ 13.8	92.4 $\pm$ 14.8	97.8 $\pm$ 12.8	88.6 $\pm$ 17	89 $\pm$ 14.1	98 $\pm$ 18.62	106 $\pm$ 15.81	89 $\pm$ 13.8	96.4 $\pm$ 14.8	100.8 $\pm$ 12.8

Data represented as mean  $\pm$  S.D., significantly different from control at <sup>a</sup> $P < .05$ ,  $n = 5$  animals per group.

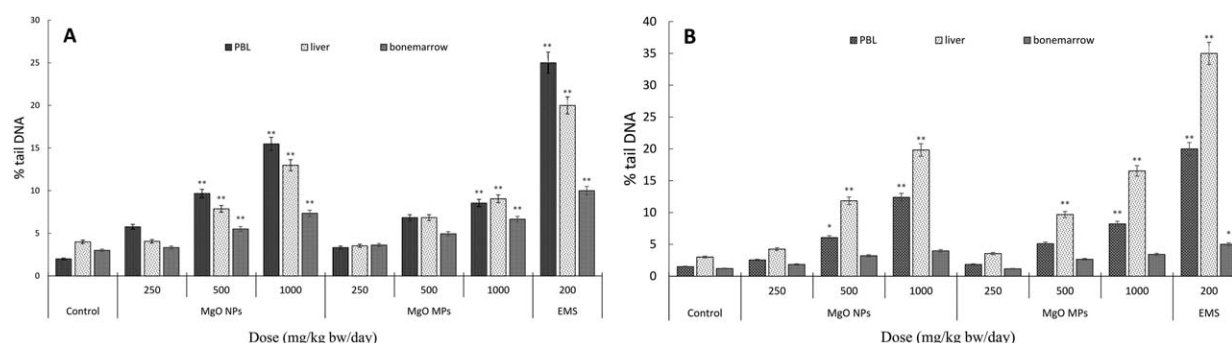


**FIGURE 3** Mean % tail DNA in (A) male (B) female Wistar rats after 28 day repeated study with different doses of MgO NPs and MPs. Milli Q water (control), EMS (positive control), Data represented as mean  $\pm$  S.D., significantly different from control at \* =  $P < .05$  and \*\* =  $P < .01$ ,  $n = 5$  animals per group

### 3.6 | Histopathological examinations

In histopathology studies, the organs were evaluated for any pathological changes in tissue morphology and anatomy as well as for the presence of any foreign deposits and contaminants. The microscopic sections, namely, liver, kidney, stomach, spleen, and brain stained with H & E were examined in the current study. Histopathological damage was found only in the stomach, liver, and kidney tissues of rats treated with 1000 mg/kg of MgO NPs. In liver, the architecture of the tissue was altered with a dilated portal tract, cellular distortions, and formation vacuoles. Further, there was disassembling of the glomerulus and swelling of renal capsules observed in kidney sections. The disrupted granular layer was found in histological sections of the stomach. However, detectable pathological changes were not detected in nano and microtreated spleen and brain tissues of male and female rats. The slides of control and nanotreated liver, kidneys, and stomach of male and female rats have been shown in Figure 4.

### 3.7 | Tissue biodistribution of magnesium particles

The biodistribution level of Mg content was estimated by ICP-OES analysis. The results revealed that Mg got accumulated in liver, kidneys,

spleen, heart, brain, whole blood tissue along with urine and feces in the micro and nanotreated rats (Figure 5). The distribution of Mg was high at 1000 followed by 500 and 250 mg/kg doses in male and female rats for both MgO NPs and MPs. The order of accumulation was liver > kidneys > spleen > blood > brain. Significant accumulation of Mg was observed in rats treated with MgO MPs at 500 and 1000 mg/kg in the liver and kidneys, whereas, in spleen and blood only at a high dose. In the 1000 mg/kg MgO NPs treated rats, a significant amount of Mg was removed via urine in a dose-dependent fashion. Similarly, Mg excreted in feces was also more at the high dose. However, MgO MPs treated rats showed statistically significant excretion of Mg in feces, probably due to their larger size of particles than nano MgO.

## 4 | DISCUSSION

Nanoparticles (NPs) with their varied physicochemical properties, elicit a wide range of physiological responses such as distribution patterns and interactions with biological molecules.<sup>28</sup> Although, particle size and surface area of the particles are important features that affect *in vivo* bio reactivity, crystal structure, purity, hydrodynamic size, and

**TABLE 3** The frequency of MN-PCEs and percent PCEs in male and female rat bone marrow and PB cells treated orally with different doses of MgO NPs and MPs for 28 days

Treatment	Dose (mg/kg bw/day)	Bone marrow cells				PB cells			
		Male		Female		Male		Female	
		MN-PCEs frequency	% PCEs	MN-PCEs frequency	% PCEs	MN-PCEs frequency	% PCEs	MN-PCEs frequency	% PCEs
Control <sup>A</sup>	Milli-Q	4.1 $\pm$ 1.3	32.0 $\pm$ 1.28	5.6 $\pm$ 1.23	32.3 $\pm$ 1.03	2.3 $\pm$ 0.62	3.7 $\pm$ 0.81	2.1 $\pm$ 1.33	3.0 $\pm$ 1.48
MgO NPs	250	4.0 $\pm$ 1.0	31.6 $\pm$ 1.96	6.0 $\pm$ 1.7	30.5 $\pm$ 1.54	3.2 $\pm$ 1.27	2.3 $\pm$ 0.36	3.8 $\pm$ 1.43	2.8 $\pm$ 0.28
	500	7.0 $\pm$ 1.0a	30.5 $\pm$ 0.40	9.0 $\pm$ 1.0a	28.5 $\pm$ 1.42	4.9 $\pm$ 1.48a	2.2 $\pm$ 0.60	4.8 $\pm$ 1.50a	2.3 $\pm$ 0.31
	1000	9.3 $\pm$ 1.23b	28.8 $\pm$ 1.4a	11.7 $\pm$ 1.3b	23.3 $\pm$ 1.41b	6.3 $\pm$ 0.47b	2.2 $\pm$ 0.58	6.8 $\pm$ 0.76b	1.9 $\pm$ 0.84
MgO MPs	250	3.7 $\pm$ 1.43	32.2 $\pm$ 1.13	4.0 $\pm$ 1.5	32.0 $\pm$ 1.8	1.9 $\pm$ 0.43	2.9 $\pm$ 0.42	1.9 $\pm$ 0.35	2.9 $\pm$ 0.53
	500	4.3 $\pm$ 1.3	30.9 $\pm$ 0.32	5.0 $\pm$ 1.2	30.6 $\pm$ 0.74	2.2 $\pm$ 0.42	2.7 $\pm$ 0.32	2.3 $\pm$ 0.81	2.7 $\pm$ 0.46
	1000	5.0 $\pm$ 1.0	30.3 $\pm$ 0.71	6.0 $\pm$ 1.1	28.4 $\pm$ 1.26	2.5 $\pm$ 0.53	2.7 $\pm$ 0.14	2.6 $\pm$ 0.40	2.5 $\pm$ 0.22
EMS <sup>B</sup>	200	22.0 $\pm$ 3.15b	21.1 $\pm$ 1.4b	30.5 $\pm$ 3.2b	22.4 $\pm$ 0.33b	13.3 $\pm$ 2.4b	1.7 $\pm$ 0.45b	12.6 $\pm$ 2.45b	1.1 $\pm$ 1.24b

Control<sup>A</sup> (Milli-Q water), EMS<sup>B</sup> (positive control), Data represented as mean  $\pm$  S.D, significantly different from control <sup>a</sup> $P < .05$  and <sup>b</sup> $P < .01$ ,  $n = 5$  animals per group.

**TABLE 4** Percent MI and total cytogenetic changes observed in bone-marrow cells of male and female Wistar rats treated repeatedly for 28 days with different doses of MgO NPs and MPs

Dose (mg/kg bw/day)		M.I. (%)		Total cytogenetic changes	
		Mean $\pm$ SD		Mean $\pm$ SD	
		Male	Female	Male	Female
Control <sup>A</sup>		4.14 $\pm$ 1.0	4.20 $\pm$ 1.01	1.66 $\pm$ 0.81	1.60 $\pm$ 0.98
MgO NPs	250	3.79 $\pm$ 1.0	3.39 $\pm$ 1.22	3.77 $\pm$ 0.31	3.24 $\pm$ 0.38
	500	3.36 $\pm$ 0.6	3.35 $\pm$ 1.16	4.95 $\pm$ 1.74b	5.27 $\pm$ 1.61a
	1000	3.23 $\pm$ 0.6	3.35 $\pm$ 1.10	8.19 $\pm$ 0.35b	7.79 $\pm$ 0.10b
MgO MPs	250	4.14 $\pm$ 1.2	4.01 $\pm$ 0.94	1.82 $\pm$ 0.35	1.73 $\pm$ 0.40
	500	3.81 $\pm$ 0.6	3.71 $\pm$ 1.33	3.18 $\pm$ 0.55	3.51 $\pm$ 0.56
	1000	3.78 $\pm$ 0.1	3.41 $\pm$ 0.60	5.85 $\pm$ 0.61	5.26 $\pm$ 0.47
EMS <sup>B</sup>		3.22 $\pm$ 0.9	3.30 $\pm$ 0.86	53.73 $\pm$ 9.0b	55.07 $\pm$ 8.1b

Control<sup>A</sup> (Milli-Q water), EMS<sup>B</sup> (200 mg/kg bw), Data represented as mean  $\pm$  S.D, Significantly different from control at <sup>a</sup> $P < .05$ , <sup>b</sup>  $P < .01$ .

Abbreviations: MI, mitotic index.

One hundred metaphases were analyzed per animal;  $n = 5$  animals per group.

aggregation nature of the NPs in aqueous media also regulate the biological response.<sup>29,30</sup> A number of studies have attempted to address the relationship between characteristic features of NPs and their physiological behavior.<sup>31–33</sup> The small size of NPs may help them in penetrating into the cells and get transferred across cell membranes and enter systemic circulation to reach the specific target sites.<sup>34,35</sup> In this study, the hydrodynamic size obtained for MgO NPs from DLS was greater than the size measured by TEM analysis which may be due to the agglomeration of the particles in the Milli Q water, which in turn depends on surface charge. Zeta potential measurement gives surface charge, by which we could anticipate stability of MgO NP in suspension.

The oral route is an important port of the entry for NPs because food products and water may possibly contain nano and microparticles (MPs).<sup>36,37</sup> Therefore, this route is the most convenient and popular route of administration for NPs toxicity assessment and there is a possibility of more frequent occurrence of ingestion of NPs in comparison to skin or inhalation exposure.<sup>38</sup> The present investigation will give the primary confirmation of the genotoxic, biochemical, and biodistribution of the Mg in different tissues, urine and feces with MgO NPs and MPs in albino Wistar male and female rats after 28 days of repeated oral treatment. The results of this study revealed that MgO NPs and MPs induced toxic effects but not death or severe suffering with the highest dose of 1000 mg/kg. The possible toxic effects that may be caused by NPs include tissue inflammation and altered cellular redox potential.<sup>39</sup> The alterations may lead to mutagenesis by causing morphological changes and damage to genetic material.<sup>40</sup> Genotoxicity is a fundamental parameter to assess the toxic effects of NPs as mankind's concern about genetic diseases and cancer is well known.<sup>27</sup> Genotoxic studies in Wistar rats with MgO NPs and MPs after 28 days exposure was assessed by a comet, MN, and CA analysis. The results of the comet assay suggested cellular DNA damage, which was expressed in terms of increased % tail DNA. The DNA damage may be due to the direct

interaction or interference of NPs in the process of DNA replication.<sup>41</sup> A significant increase in bone marrow MN-PCE and decrease in % PCE was observed with the MNT in NP treated animals. The decrease in % PCE indicated that cell death had occurred in the treated groups. It is possible that clastogenic events are involved in the formation of these MN.<sup>42</sup> Cytogenetic analysis of bone marrow cells in nano and micro treated rats showed an increased number of CAs and decreasing MI. These abnormalities may be due to the hindrance of cell cycle progression.<sup>43</sup> The mechanisms responsible for the genotoxicity of NPs involve oxidative stress which causes redox imbalance within cells usually as a result of an increase in intracellular ROS. Generated ROS in the metabolizing cells could attack DNA base guanine and form 8-OHdG lesions, which are known to have a mutagenic potential.<sup>44</sup> A few studies with metal oxide NPs for genotoxicity analysis upon repeated dose exposure regimens documented similar findings to our results.<sup>44–47</sup> Biochemical enzymes and their physiological levels serve as a preliminary diagnosis tool for the assessing pathological condition or alteration upon entry of xenobiotics.<sup>48</sup> The liver is an important site for NP deposition and may cause changes in the serum enzymatic composition. The elevated levels of serum proteins and the enzyme levels are good indicators of hepatocellular injury, inflammation, kidney function impairment, and cholestasis.<sup>49</sup> In this study, it was observed that MgO NPs and MPs significantly enhanced the enzyme levels of ALP, AST, and ALT in serum as well as liver and kidney homogenates of treated rats and was dose but not gender dependent. Increased levels of these enzymes in the tissue homogenates may be due to the extent of hepatocellular injury leading to possible leakage of these enzymes into the bloodstream.<sup>50,51</sup> A study by Easo et al.<sup>52</sup> reported functional integrity of cell membrane would be lost resulting in perturbation of transport function of hepatocytes causes tissue necrosis. Similar alterations of ALP, AST, and ALT were observed with other metal NPs.<sup>44,53–55</sup> In this study, we have investigated several oxidative stress parameters such as MDA, LDH, GSH, and CAT in liver and kidney homogenates of MgO NPs and





TABLE 7 Effects of MgO NPs and MPs in kidney oxidative stress parameters in male and female Wistar rats treated orally after 28-day repeated exposure

Dose (mg/kg bw/day)	GSH ( $\mu\text{g/g}$ )		Catalase (U/mg protein)		MDA (nmol/g)		LDH (U/mg protein)		ALP (U/mg protein)	
	Male	Female	Male	Female	Male	Female	Male	Female	Male	Female
Controla	8.43 $\pm$ 2.3	9.06 $\pm$ 2.1	200.5 $\pm$ 15.25	198.5 $\pm$ 17.35	6.45 $\pm$ 2.25	6.5 $\pm$ 2.5	239 $\pm$ 10.25	240 $\pm$ 10.5	21.4 $\pm$ 2.36	22.21 $\pm$ 2.44
NPs										
250	7.42 $\pm$ 2.05	7.16 $\pm$ 2.3	185.5 $\pm$ 15.65	182.14 $\pm$ 16.25	7.25 $\pm$ 2.3	7.32 $\pm$ 2.45	255 $\pm$ 11.32	252 $\pm$ 11.52	22.8 $\pm$ 2.44	26.52 $\pm$ 2.65
500	5.62 $\pm$ 2.43	5.6 $\pm$ 2.5a	158.2 $\pm$ 16.4a	149.6 $\pm$ 17.2a	8.95 $\pm$ 2.55	9.28 $\pm$ 2.88	265 $\pm$ 12.65a	271 $\pm$ 12.5a	25.4 $\pm$ 2.75	29.84 $\pm$ 3.2b
1000	4.28 $\pm$ 2.34a	3.58 $\pm$ 2.25b	125.4 $\pm$ 15.2a	122.6 $\pm$ 16.4b	9.25 $\pm$ 2.85	10.74 $\pm$ 2.6a	288 $\pm$ 12.35b	296 $\pm$ 14.35b	28.2 $\pm$ 2.32b	32.2 $\pm$ 3.44b
MPs										
250	7.56 $\pm$ 2.15	7.58 $\pm$ 2.42	192.2 $\pm$ 17.25	189.6 $\pm$ 17.5	6.85 $\pm$ 2.35	6.65 $\pm$ 2.5	245 $\pm$ 11.35	252 $\pm$ 12.34	21.6 $\pm$ 2.66	21.91 $\pm$ 2.25
500	6.35 $\pm$ 2.4	6.15 $\pm$ 2.1	173.4 $\pm$ 17.5a	165.4 $\pm$ 17.6a	7.65 $\pm$ 2.28	8.23 $\pm$ 2.44	259 $\pm$ 12.28a	261 $\pm$ 11.25a	23.8 $\pm$ 2.48	23.65 $\pm$ 2.16
1000	5.16 $\pm$ 2.35	5.04 $\pm$ 2.15a	138.3 $\pm$ 15.45b	136.8 $\pm$ 15.8b	8.37 $\pm$ 2.39	9.25 $\pm$ 2.42	265 $\pm$ 12.64a	277 $\pm$ 12.36b	25.5 $\pm$ 2.54	24.52 $\pm$ 2.24

Control (Milli-Q water). Data represented as mean  $\pm$  S.D, significantly different from control at <sup>a</sup> $p < .05$ , <sup>b</sup> $p < .01$ .  $n = 5$  animals per group.

MPs treated rats. Interactions of NPs with proteins and enzymes may have resulted in the production of ROS due to interference with antioxidant defenses leading to induction of oxidative stress.<sup>56–59</sup> This study illustrates that a significant increase in MDA and LDH and depletion in GSH and CAT levels was observed in the tissue homogenates at a high dose of NPs indicating free radical generation. The elevated levels of MDA indicate the formation of hydroxyl radicals which in turn is associated with lipid membrane of tissue that may have led to inactivation of the enzymes by cross linking with MDA, which might have caused an increase in accumulation of ROS that could contribute to the inhibition of metabolic process and the onset of lesions in vital organs.<sup>60,61</sup> Our results illustrated a dose dependent depletion of GSH, possibly due to enhanced utilization in both enzymatic and nonenzymatic reactions. Individual antioxidant enzymes play different strategic roles to counteract oxidant insult. In this study, a significant increase in CAT in NP treated rat tissues was observed. Superoxide radicals in association with adventitious metal like Mg triggers the oxidative damage of proteins, lipids and nucleic acids.<sup>62</sup> MgO NPs and MPs treatment caused an elevation in CAT levels as a defensive mechanism against excess  $\text{H}_2\text{O}_2$  levels. Depleted GSH levels suggest increased utilization of GSH in conjugation reactions as part of detoxification mechanism thus supporting ROS mediated molecular mechanism. Hence, it is suggested that MDA, CAT, and GSH levels are good biomarkers in assessing toxicity. Material composition and surface characteristics with subsequent cellular damage could be the source of NP-induced toxicity via cell activation and ROS production.<sup>63–65</sup> Altered antioxidant status as reported in our study is supported by findings from other investigations.<sup>42,53,66</sup>

The histopathological examination of the vital organs may be helpful in detecting pathological changes in tissues of rats treated with MgO NPs and MPs. The results showed remarkable morphological alterations like dilated portal tract and vacuoles in liver, disassembling of the glomerulus, swelling of renal capsules in tissue sections of kidney and glandular distortion of the stomach linings, which were prominent at high doses of NPs in male and female rats. A study reported liver injury with Ag-NPs via mild infiltration of inflammatory cells in Kupffer cells.<sup>67</sup> Kupffer cells have a high tendency for the recognition and clearance of xenobiotic substances.<sup>68</sup> Therefore, the increased number of Kupffer cells may be attributed to the ability of NPs to evoke the immune responses and enable their clearance.<sup>69</sup> The observed hepatic necrosis may be attributed to the overproduction of ROS, which caused an impairment of the endogenous antioxidant system, with a subsequent increase in the lipid peroxidation associated cellular damage.<sup>70</sup> A study by Sardari et al.<sup>71</sup> reported necrosis of glomerular cells, the Bowman's capsule and proximal tubular cells in the kidney in rats after administration of silver NPs for 30 days.

The hematological profile was assessed to examine the physiological state after 28 days exposure to MgO NPs and MPs at different doses. It was found that the rats treated with high dose of NPs showed a significant decrease in HGB, RBC, PLT, and HCT. Further, significant increase in WBC was also evident. The changes might be due to the interference of NPs in hematopoiesis and activation of innate defense system.<sup>72–74</sup> In accordance with this study, a raise in levels of RBC,

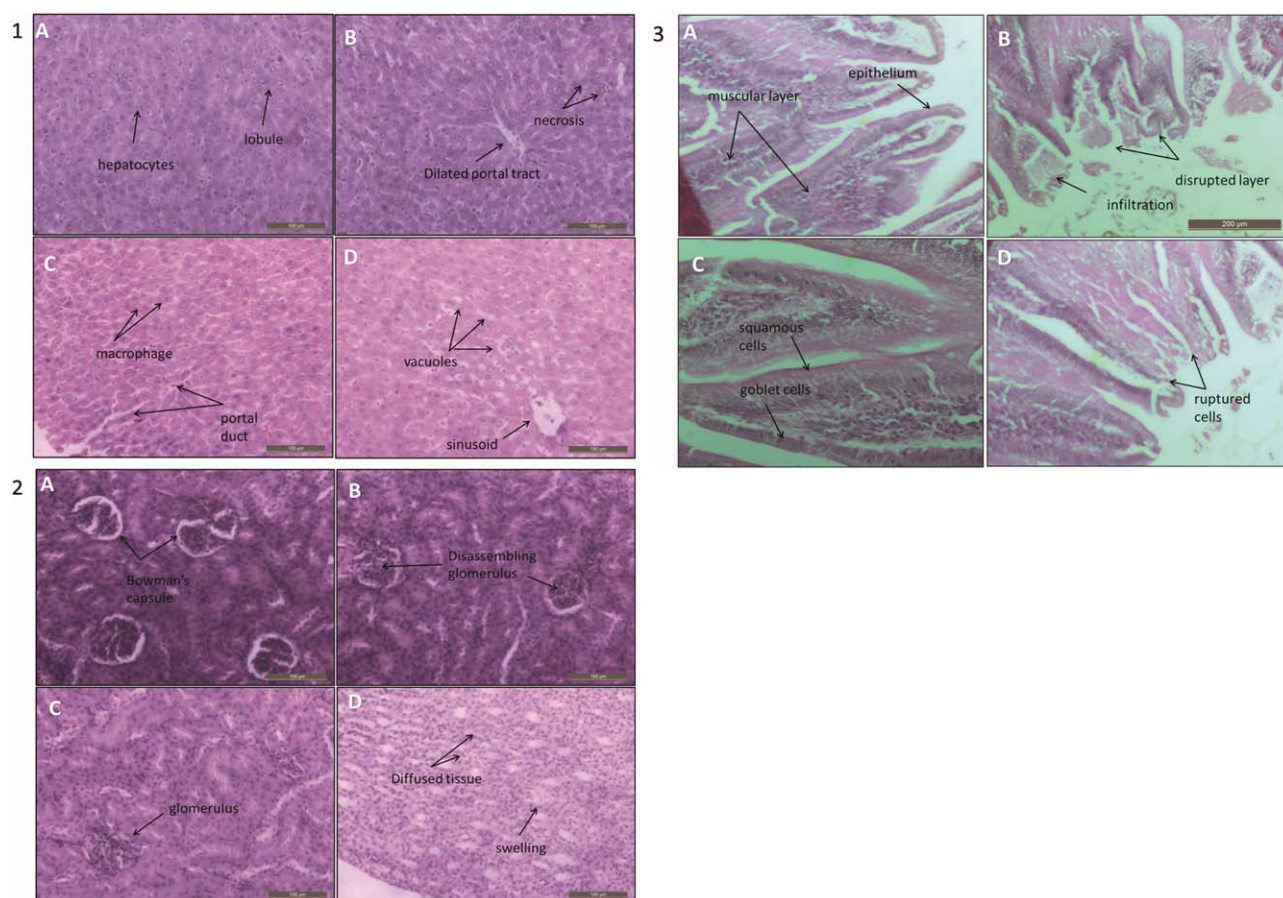


**FIGURE 4** Histopathological examination of (1) liver, (2) kidneys, (3) stomach lining tissues of control (A and C), and exposed to MgO NPs (1000 mg/kg bw/day; B and D) of male and female rats for 28 days. The tissues were isolated and fixed; the sections were stained with H & E and then examined under microscope at  $\times 400$  magnification. (Alteration is indicated by arrow). [Color figure can be viewed at [wileyonlinelibrary.com](http://wileyonlinelibrary.com)]

HGB, and HCT was reported by Espinosa-Cristobal et al.<sup>75</sup> Increases in these blood parameters suggest a higher need for oxygen transport in these animals thus disrupting the normal cell physiology.<sup>76</sup>

The biodistribution study after 28 day exposure with MgO NPs and MPs in male and female Wistar rats revealed significant Mg content in various tissues by ICP-OES analysis. Tissue biodistribution studies revealed NPs rapidly distribute from the systemic circulation to all tissues.<sup>77</sup> Mg ions could be released from NPs and MPs treated rats may pass through the gastrointestinal barrier and accumulate in various organs and tissues. The amount of absorption of Mg ions increased as the dose administered was raised. Moreover, the distribution pattern was dose dependent but not gender. The size of particles has been proven to influence their behavior. In general, the particles with smaller size have a wider tissue distribution, easily get internalized within the body to a greater extent and have a larger toxic potency.<sup>78,79</sup> The current data revealed significant Mg content in liver, kidneys, spleen, blood, heart, and brain along with urine and feces. The maximum accumulation was in liver of MgO NP treated rats followed by kidneys in both the sexes. This could be due to biotransformation in the liver and excretion by the kidneys *in vivo*. The kidney tissue has been identified as a potential target of NP toxicity after liver.<sup>58,80</sup> The higher quantity of Mg ions from NP dosed rats was excreted via urine due to the larger

orifice diameter of the glomerulus during the filtration. However, rats receiving MgO MPs revealed that large quantities of Mg could pass through the intestinal barrier and get quickly excreted via feces because of their large size. The excretion of the Mg ions was greater in feces of MP-treated rats in contrast to NP-treated rats. It can be summarised that characteristic features of NPs could have an influence on the toxicokinetic properties.<sup>81</sup> The *in vivo* toxicity of NPs was directly connected to the biodistribution and bioaccumulation and closely linked with the size associated capacity.<sup>35</sup> In concurrence with this study, several investigations also reported similar results with various NPs.<sup>79,82–84</sup>

To our knowledge, this is the first study showing that MgO NPs and MPs induced genotoxicity in rats. However, the exact mechanism of NP induced genotoxicity is still unknown. Therefore, considering the widespread increasing commercial applications of these MgO NPs should be regarded with concern.

## 5 | CONCLUSION

Physicochemical properties of MgO NPs played a crucial role in inducing toxicity, as the NPs produced prominent toxic effects in comparison to MPs. It can be concluded that MgO NPs induced genotoxicity in



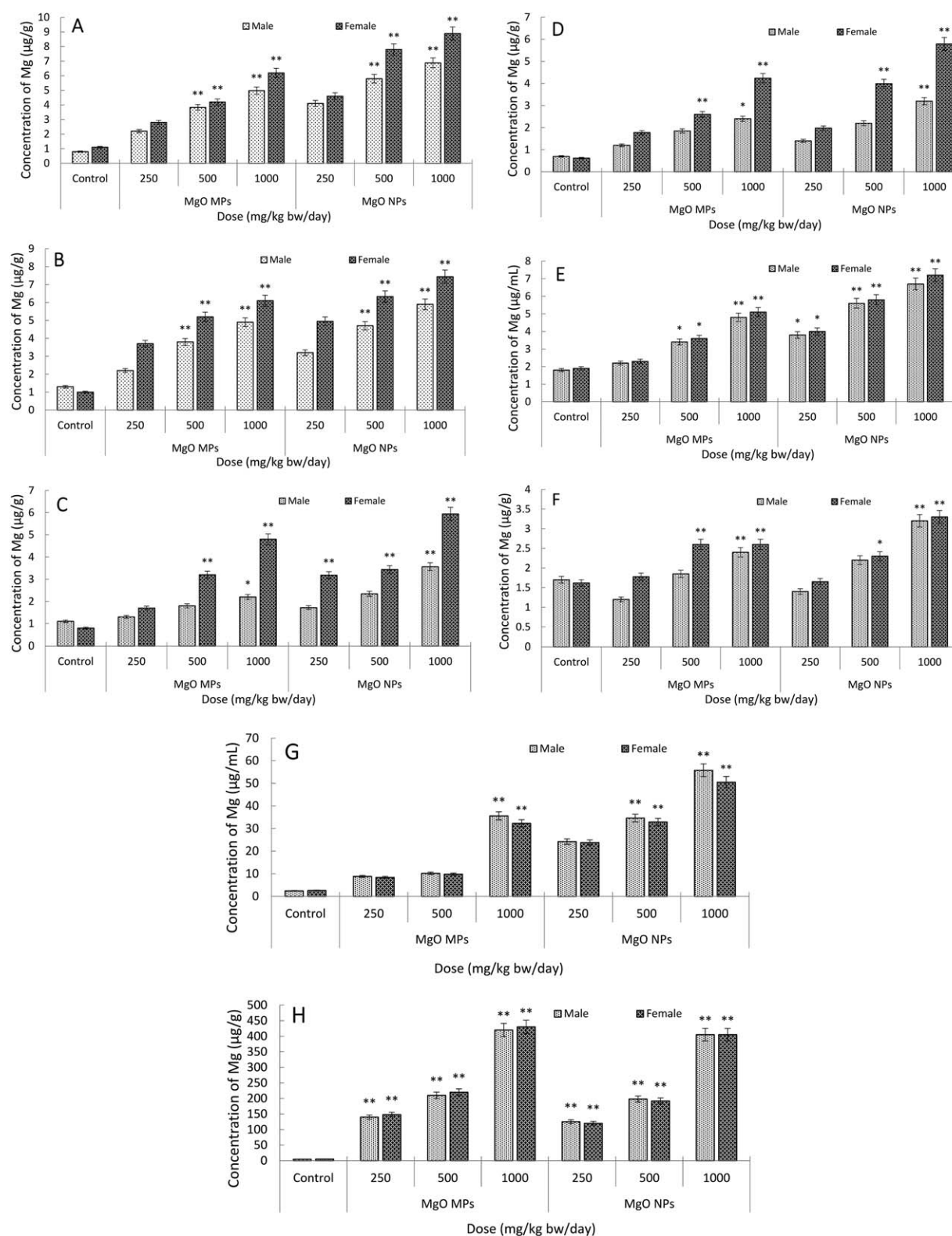


**FIGURE 5** Tissue distribution of Magnesium measured by ICP-OES in (A) liver, (B) kidneys, (C) spleen, (D) heart, (E) blood, (F) brain, (G) urine, and (H) feces of rats after 28 day repeated oral administration of 250, 500, and 1000 mg/kg bw/day of MgO NPs and MPs. Significantly different from control at \* =  $P < .05$  and \*\* =  $P < .01$ ,  $n = 5$  animals per group

dose dependent manner, which was significant at the high dose level. The occurrence of DNA damage, micronucleus formation, and chromosomal changes might be the evidence for this effect. Our study has

provided evidence that MgO NPs was able to induce changes in the activities of the biochemical enzymes. Repeated exposure of this compound may lead to alterations of enzymes in the vital organs. It is also

suggested that these enzymes are good biomarkers for studies of toxic insult or tissue injury as it is ubiquitously present in all important tissues and their levels are indicative of tissue necrosis. Moreover, the biodistribution pattern revealed that the maximum accumulation of Mg content was in the liver. This study does not imply that of MgO NPs/MPs should be avoided in the diverse fields. It is a preliminary study, which revealed the consequences of repeated exposure to high levels of MgO NPs and MPs. Further studies are needed to understand the exact mechanism of toxicity by which biochemical pathway of these particles is inducing toxicity.

## ACKNOWLEDGMENTS

The authors express their sincere thanks to the Director IICT, Hyderabad for providing funds and facilities to execute this study. They greatly acknowledge the help of analytical division of our institute for the characterization and biodistribution studies. The authors are thankful to Dr. M.F. Rahman and Dr. M. Mahboob (Principal Technical Officers, Pharmacology and Toxicology Division) for their help in the determination of haematological and biochemical parameters. Bhanuramya Mangalampalli (SRF) is grateful to University Grants Commission. Further, Dr. Paramjit Grover (CSIR-Emeritus Scientist) and Naresh Dumala (SRF) are grateful to Council of Scientific and Industrial Research, India for the award of fellowships, respectively.

## CONFLICT OF INTEREST

There is no conflict of interest related to this research.

## ORCID

Paramjit Grover  <http://orcid.org/0000-0002-1928-8273>

## REFERENCES

- [1] Krishnamoorthy K, Moon JY, Hyun HB, Cho SK, Kim S-J. Mechanistic investigation on the toxicity of MgO nanoparticles toward cancer cells. *J Mater Chem*. 2012;22(7):24610.
- [2] Moorthy SK, Ashok C, Rao KV, Viswanathan C. Synthesis and characterization of MgO nanoparticles by Neem leaves through green method. *Mater Today: Proc*. 2015;2(9):4360–4368.
- [3] Patel MK, Agrawal VV, Malhotra BD, Ansari S. Nanostructured magnesium oxide: a suitable material for DNA based biosensors. *Mater Focus*. 2014;3(1):1–11.
- [4] Ge S, Wang G, Shen Y, et al. Cytotoxic effects of MgO nanoparticles on human umbilical vein endothelial cells in vitro. *IET Nanobio-technol*. 2011;5(2):36–40.
- [5] Sun J, Wang S, Zhao D, Hun FH, Weng L, Liu H. Cytotoxicity, permeability, and inflammation of metal oxide nanoparticles in human cardiac microvascular endothelial cells. *Cell Biol Toxicol*. 2011;27(5):333–342.
- [6] Lai JC, Lai MB, Jandhyam S, et al. Exposure to titanium dioxide and other metallic oxide nanoparticles induces cytotoxicity on human neural cells and fibroblasts. *Int J Nanomed*. 2008;3(4):533.
- [7] Kumaran RS, Choi Y-K, Singh V, et al. In vitro cytotoxic evaluation of MgO nanoparticles and their effect on the expression of ROS genes. *Int J Mol Sci*. 2015;16(4):7551–7564.
- [8] Mangalampalli B, Dumala N, Grover P. Acute oral toxicity study of magnesium oxide nanoparticles and microparticles in female albino Wistar rats. *Regul Toxicol Pharmacol*. 2017;90:170–184.
- [9] Gelli K, Porika M, Anreddy RNR. Assessment of pulmonary toxicity of MgO nanoparticles in rats. *Environ Toxicol*. 2015;30(3):308–314.
- [10] Kiranmai G, Reddy ARN. Antioxidant status in MgO nanoparticle-exposed rats. *Toxicol Ind Health*. 2013;29(10):897–903.
- [11] Burleson W, Picard R. Affective agents: Sustaining motivation to learn through failure and a state of stuck. In: Proceedings of the ITS Workshop on Social and Emotional Intelligence in Learning Environments. Maceio, Brasil; 2004.
- [12] Ju-Nam Y, Lead JR. Manufactured nanoparticles: an overview of their chemistry, interactions and potential environmental implications. *Sci Total Environ*. 2008;400(1–3):396–414.
- [13] Hanot-Roy M, Tubeuf E, Guilbert A, et al. Oxidative stress pathways involved in cytotoxicity and genotoxicity of titanium dioxide (TiO<sub>2</sub>) nanoparticles on cells constitutive of alveolo-capillary barrier in vitro. *Toxicol In Vitro*. 2016;33:125–135.
- [14] Shrivastava R, Kushwaha P, Bhutia YC, Flora S. Oxidative stress following exposure to silver and gold nanoparticles in mice. *Toxicol Ind Health*. 2016;32(8):1391–1404.
- [15] OECD. Test No. 407: Repeated Dose 28-Day Oral Toxicity Study in Rodents. Paris: OECD Publishing; 1995.
- [16] OECD. Test No. 489: In Vivo Mammalian Alkaline Comet Assay. Paris: OECD Publishing; 2014.
- [17] Tice R, Agurell E, Anderson D, et al. Single cell gel/comet assay: guidelines for in vitro and in vivo genetic toxicology testing. *Environ Mol Mutagen*. 2000;35(3):206–221.
- [18] Pool-Zobel BL, Lotzmann N, Knoll M, et al. Detection of genotoxic effects in human gastric and nasal mucosa cells isolated from biopsy samples. *Environ Mol Mutagen*. 1994;24(1):23–45.
- [19] OECD. Test No. 474: Mammalian Erythrocyte Micronucleus Test. Paris: OECD Publishing; 2014.
- [20] Schmid W. The micronucleus test. *Mutat Res*. 1975;31(1):9–15.
- [21] OECD Guidelines for Testing of Chemicals, Organization for Economic Cooperation and Development. Test No. 475: Mammalian Bone Marrow Chromosome Aberration Test. Paris: OECD Publishing; 1997.
- [22] Yatzidis H. Measurement of transaminases in serum. *Nature*. 1960;186:79–80.
- [23] Jollow D, Mitchell J, Zampaglione N, Gillette J. Bromobenzene-induced liver necrosis. Protective role of glutathione and evidence for 3, 4-bromobenzene oxide as the hepatotoxic metabolite. *Pharmacology*. 1974;11(3):151–169.
- [24] McQueen M. Optimal assay of LDH and  $\alpha$ -HBD at 37° C. *Ann Clin Biochem*. 1972;9(1–6):21–25.
- [25] Ohkawa H, Ohishi N, Yagi K. Assay for lipid peroxides in animal tissues by thiobarbituric acid reaction. *Anal Biochem*. 1979;95(2):351–358.
- [26] Sinha AK. Colorimetric assay of catalase. *Anal Biochem*. 1972;47(2):389–394.
- [27] Dumala N, Mangalampalli B, Chinde S, et al. Genotoxicity study of nickel oxide nanoparticles in female Wistar rats after acute oral exposure. *Mutagenesis*. 2017;32(4):417–427.
- [28] Li N, Georas S, Alexis N, et al. A work group report on ultrafine particles (American Academy of Allergy, Asthma & Immunology): why ambient ultrafine and engineered nanoparticles should receive special attention for possible adverse health outcomes in human subjects. *J Allergy Clin Immunol*. 2016;138(2):386–396.
- [29] Nel AE, Mädler L, Velegol D, et al. Understanding biophysicochemical interactions at the nano-bio interface. *Nat Mater*. 2009;8(7):543–557.



- [30] Sendra M, Yeste P, Moreno-Garrido I, Gatica J, Blasco J. CeO<sub>2</sub> NPs, toxic or protective to phytoplankton? Charge of nanoparticles and cell wall as factors which cause changes in cell complexity. *Sci Total Environ*. 2017;590–591:304–315.
- [31] Hartmann DL. *Global physical climatology*. Oxford, United Kingdom: Newnes; 2015.
- [32] Murdock RC, Braydich-Stolle L, Schrand AM, Schlager JJ, Hussain SM. Characterization of nanomaterial dispersion in solution prior to in vitro exposure using dynamic light scattering technique. *Toxicol Sci*. 2008;101(2):239–253.
- [33] Stefaniak AB, Hackley VA, Roebben G, et al. Nanoscale reference materials for environmental, health and safety measurements: needs, gaps and opportunities. *Nanotoxicology*. 2013;7(8):1325–1337.
- [34] Gheshlaghi ZN, Riazi GH, Ahmadian S, Ghafari M, Mahinpour R. Toxicity and interaction of titanium dioxide nanoparticles with microtubule protein. *Acta Biochim Biophys Sin*. 2008;40(9):777–782.
- [35] Shang L, Nienhaus K, Nienhaus GU. Engineered nanoparticles interacting with cells: size matters. *J Nanobiotechnol*. 2014;12:5.
- [36] Powell JJ, Faria N, Thomas-McKay E, Pele LC. Origin and fate of dietary nanoparticles and microparticles in the gastrointestinal tract. *J Autoimmun*. 2010;34(3):J226–JJ33.
- [37] Lomer MC, Thompson RP, Powell JJ. Fine and ultrafine particles of the diet: influence on the mucosal immune response and association with Crohn's disease. *Proc Nutr Soc*. 2002;61(1):123–130.
- [38] Rashidi L, Khosravi-Darani K. The applications of nanotechnology in food industry. *Crit Rev Food Sci Nutr*. 2011;51(8):723–730.
- [39] Colvin VL. The potential environmental impact of engineered nanomaterials. *Nat Biotechnol*. 2003;21(10):1166–1170.
- [40] Magaye R, Zhao J, Bowman L, Ding M. Genotoxicity and carcinogenicity of cobalt-, nickel- and copper-based nanoparticles (Review). *Exp Ther Med*. 2012;4(4):551–561.
- [41] An F, Bai J, Balantekin A, et al. Observation of electron-antineutrino disappearance at Daya Bay. *Phys Rev Lett*. 2012;108(17):171803.
- [42] Singh SP, Kumari M, Kumari SI, Rahman MF, Mahboob M, Grover P. Toxicity assessment of manganese oxide micro and nanoparticles in Wistar rats after 28 days of repeated oral exposure. *J Appl Toxicol*. 2013;33(10):1165–1179.
- [43] Setyawati MI, Tay CY, Docter D, Stauber RH, Leong DT. Understanding and exploiting nanoparticles' intimacy with the blood vessel and blood. *Chem Soc Rev*. 2015;44(22):8174–8199.
- [44] Kumari M, Rajak S, Singh SP, et al. Repeated oral dose toxicity of iron oxide nanoparticles: biochemical and histopathological alterations in different tissues of rats. *J Nanosci Nanotechnol*. 2012;12(3):2149–2159.
- [45] Sharma V, Singh P, Pandey AK, Dhawan A. Induction of oxidative stress, DNA damage and apoptosis in mouse liver after sub-acute oral exposure to zinc oxide nanoparticles. *Mutat Res*. 2012;745(1–2):84–91.
- [46] Singh SP, Chinde S, Kamal SSK, Rahman M, Mahboob M, Grover P. Genotoxic effects of chromium oxide nanoparticles and microparticles in Wistar rats after 28 days of repeated oral exposure. *Environ Sci Pollut Res*. 2016;23(4):3914–3924.
- [47] Kim YS, Kim JS, Cho HS, et al. Twenty-eight-day oral toxicity, genotoxicity, and gender-related tissue distribution of silver nanoparticles in Sprague-Dawley rats. *Inhal Toxicol*. 2008;20(6):575–583.
- [48] Kim JH, Kim JH, Kim K-W, Kim MH, Yu YS. Intravenously administered gold nanoparticles pass through the blood-retinal barrier depending on the particle size, and induce no retinal toxicity. *Nanotechnology*. 2009;20(50):505101.
- [49] Quimby FW. *The Clinical Chemistry of Laboratory Animals*. Philadelphia: Taylor & Francis; 1999.
- [50] Abdelhalim MAK. Uptake of gold nanoparticles in several rat organs after intraperitoneal administration in vivo: a fluorescence study. *Biomed Res Int*. 2013;2013:353695.
- [51] Kumari M, Kumari SI, Grover P. Genotoxicity analysis of cerium oxide micro and nanoparticles in Wistar rats after 28 days of repeated oral administration. *Mutagenesis*. 2014;29(6):467–479.
- [52] Easo SL, Mohanan P. Hepatotoxicity evaluation of dextran stabilized iron oxide nanoparticles in Wistar rats. *Int J Pharm*. 2016;509(1–2):28–34.
- [53] Chinde S, Grover P. Toxicological assessment of nano and micron-sized tungsten oxide after 28 days repeated oral administration to Wistar rats. *Mutat Res*. 2017;819:1.
- [54] Liu H, Ma L, Zhao J, et al. Biochemical toxicity of nano-anatase TiO<sub>2</sub> particles in mice. *Biol Trace Elem Res*. 2009;129(1–3):170–180.
- [55] Park E-J, Bae E, Yi J, et al. Repeated-dose toxicity and inflammatory responses in mice by oral administration of silver nanoparticles. *Environ Toxicol Pharmacol*. 2010;30(2):162–168.
- [56] Jain A, Ranjan S, Dasgupta N, Ramalingam C. Nanomaterials in food and agriculture: an overview on their safety concerns and regulatory issues. *Crit Rev Food Sci Nutr*. 2016;00:1–21.
- [57] Manke A, Wang L, Rojanasakul Y. Mechanisms of nanoparticle-induced oxidative stress and toxicity. *Biomed Res Int*. 2013;2013:2013.
- [58] Xue Y, Zhang T, Zhang B, Gong F, Huang Y, Tang M. Cytotoxicity and apoptosis induced by silver nanoparticles in human liver HepG2 cells in different dispersion media. *J Appl Toxicol*. 2016;36(3):352–360.
- [59] Akhtar MJ, Ahamed M, Alhadlaq HA, Alshamsan A. Nanotoxicity of cobalt induced by oxidant generation and glutathione depletion in MCF-7 cells. *Toxicol In Vitro*. 2017;40:94–101.
- [60] Avalos A, Haza AI, Mateo D, Morales P. Cytotoxicity and ROS production of manufactured silver nanoparticles of different sizes in hepatoma and leukemia cells. *J Appl Toxicol*. 2014;34(4):413–423.
- [61] Gaharwar US, Meena R, Rajamani P. Iron oxide nanoparticles induced cytotoxicity, oxidative stress and DNA damage in lymphocytes. *J Appl Toxicol*. 2017;37(10):1232–1244.
- [62] Chevion M. A site-specific mechanism for free radical induced biological damage: the essential role of redox-active transition metals. *Free Radic Biol Med*. 1988;5(1):27–37.
- [63] Lovrić J, Cho SJ, Winnik FM, Maysinger D. Unmodified cadmium telluride quantum dots induce reactive oxygen species formation leading to multiple organelle damage and cell death. *Chem Biol*. 2005;12(11):1227–1234.
- [64] Xia Q, Li H, Xiao K. Factors affecting the pharmacokinetics, biodistribution and toxicity of gold nanoparticles in drug delivery. *Curr Drug Metab*. 2016;17(9):849–861.
- [65] Wang F, Gao F, Lan M, Yuan H, Huang Y, Liu J. Oxidative stress contributes to silica nanoparticle-induced cytotoxicity in human embryonic kidney cells. *Toxicol In Vitro*. 2009;23(5):808–815.
- [66] Reddy UA, Prabhakar P, Mahboob M. Biomarkers of oxidative stress for in vivo assessment of toxicological effects of iron oxide nanoparticles. *Saudi J Biol Sci*. 2017;24(6):1172–1180.
- [67] Patlolla AK, Hackett D, Tchounwou PB. Silver nanoparticle-induced oxidative stress-dependent toxicity in Sprague-Dawley rats. *Mol Cell Biochem*. 2015;399(1–2):257–268.
- [68] Garnett MC, Kallinteri P. Nanomedicines and nanotoxicology: some physiological principles. *Occup Med*. 2006;56(5):307–311.
- [69] Yen F-L, Wu T-H, Lin L-T, Cham T-M, Lin C-C. Naringenin-loaded nanoparticles improve the physicochemical properties and the hepatoprotective effects of naringenin in orally-administered rats with CCl<sub>4</sub>-induced acute liver failure. *Pharm Res*. 2009;26(4):893–902.

- [70] Ahmad J, Ahamed M, Akhtar MJ, et al. Apoptosis induction by silica nanoparticles mediated through reactive oxygen species in human liver cell line HepG2. *Toxicol Appl Pharmacol*. 2012;259(2):160–168.
- [71] Sardari RRR, Zarchi SR, Talebi A, et al. Toxicological effects of silver nanoparticles in rats. *Afr J Microbiol Res*. 2012;6:5587–5593.
- [72] Gui S, Zhang Z, Zheng L, et al. Molecular mechanism of kidney injury of mice caused by exposure to titanium dioxide nanoparticles. *J Hazard Mater*. 2011;195:365–370.
- [73] Morsy GM, El-Ala KS, Ali AA. Studies on fate and toxicity of nanoalumina in male albino rats: Some haematological, biochemical and histological aspects. *Toxicol Ind Health*. 2016;32(4):634–655.
- [74] Shukla RK, Sharma V, Pandey AK, Singh S, Sultana S, Dhawan A. ROS-mediated genotoxicity induced by titanium dioxide nanoparticles in human epidermal cells. *Toxicol In Vitro*. 2011;25(1):231–241.
- [75] Espinosa-Cristobal L, Martinez-Castanon G, Loyola-Rodriguez J, et al. Toxicity, distribution, and accumulation of silver nanoparticles in Wistar rats. *J Nanoparticle Res*. 2013;15(6):1702.
- [76] Hadrup N, Lam HR. Oral toxicity of silver ions, silver nanoparticles and colloidal silver—a review. *Regul Toxicol Pharmacol*. 2014;68(1):1–7.
- [77] Geraets L, Oomen AG, Krystek P, et al. Tissue distribution and elimination after oral and intravenous administration of different titanium dioxide nanoparticles in rats. *Part Fibre Toxicol*. 2014;11:30.
- [78] Kermanizadeh A, Balharry D, Wallin H, Loft S, Møller P. Nanomaterial translocation—the biokinetics, tissue accumulation, toxicity and fate of materials in secondary organs—a Review. *Crit Rev Toxicol*. 2015;45(10):837–872.
- [79] Khlebtsov N, Dykman L. Biodistribution and toxicity of engineered gold nanoparticles: a review of in vitro and in vivo studies. *Chem Soc Rev*. 2011;40(3):1647–1671.
- [80] Teodoro JS, Silva R, Varela AT, et al. Low-dose, subchronic exposure to silver nanoparticles causes mitochondrial alterations in Sprague–Dawley rats. *Nanomedicine*. 2016;11(11):1359–1375.
- [81] Choi S-J, Choy J-H. Biokinetics of zinc oxide nanoparticles: toxicokinetics, biological fates, and protein interaction. *Int J Nanomed*. 2014;9:261–269.
- [82] Dziendzikowska K, Gromadzka-Ostrowska J, Lankoff A, et al. Time-dependent biodistribution and excretion of silver nanoparticles in male Wistar rats. *J Appl Toxicol*. 2012;32(11):920–928.
- [83] Loeschner K, Hadrup N, Qvortrup K, et al. Distribution of silver in rats following 28 days of repeated oral exposure to silver nanoparticles or silver acetate. *Part Fibre Toxicol*. 2011;8:18.
- [84] van der Zande M, Vandebriel RJ, Van Doren E, et al. Distribution, elimination, and toxicity of silver nanoparticles and silver ions in rats after 28-day oral exposure. *ACS Nano*. 2012;6(8):7427–7442.

**How to cite this article:** Mangalampalli B, Dumala N, Perumalla Venkata R, Grover P. Genotoxicity, biochemical, and biodistribution studies of magnesium oxide nano and microparticles in albino wistar rats after 28-day repeated oral exposure. *Environmental Toxicology*. 2018;33:396–410. <https://doi.org/10.1002/tox.22526>